THE JOURNAL OF PHYSICAL CHEMISTRY B

Article

pubs.acs.org/JPCB

Evidence for Two New Solution States of Ubiquitin by IMS−MS Analysis

Huilin Shi and David E. Clemmer*

Department of Chemistry, Indiana University, 800 Kirkwood Avenue, Bloomington, Indiana 47405, United States

ABSTRACT: Ion mobility spectrometry coupled with mass spectrometry (IMS−MS) is used to investigate the populations of different states for ubiquitin in water:methanol solutions. In these experiments, ubiquitin is electrosprayed from 20 water:methanol (100:0 to 5:95, pH = 2) solutions, ranging from native to denaturing conditions. With an increased percentage of methanol in solution, ubiquitin ions ($[M + 7H]^{7+}$ to $[M + 12H]^{12+}$) show substantial variations in both charge state distributions and ion mobility distributions. Analysis of these data provides evidence for the existence of five ubiquitin states in solution: the native N state, favored in solutions of 100:0 to 70:30 water:methanol for the +7 and +8 charge states; the more helical A state and a new closely related A′ state, favored in solutions of 70:30 to 5:95 water:methanol for the +9 to +12 charge states; the unfolded U state, populated in 40:60 to 5:95 water:methanol solutions for the +8 to +10 and +12 charge states; and a new low-abundance state termed the B state, observed for 100:0 to 70:30 water:methanol solutions in the +8 to +10 and +12 charge states. The relative abundances for different states in different solutions are determined. The analysis presented here provides insight into how solution structures evolve into anhydrous conformations and demonstrates the utility of IMS−MS methods as a means of characterizing populations of conformers for proteins in solution.

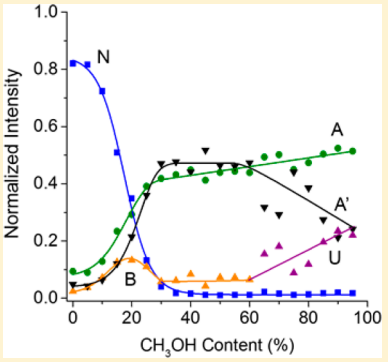

INTRODUCTION

Characterization of protein structure and conformational dynamics is key for understanding how such molecules function.[1,2] In recent years, mass spectrometry (MS) has emerged as a means of characterizing the structures of biomolecules.[3−6] For example, a protein's solution structure influences its ion charge state distribution, such that unfolded conformations carry a larger number of charges than the compact forms.[7,8] Unlike traditional structural determination techniques such as X-ray crystallography and nuclear magnetic resonance (NMR) spectroscopy, MS methods require only trace amounts of sample, and complex mixtures can be studied directly.[9,10] To acquire more detailed structural information, other experimental approaches such as ion mobility spectrometry (IMS),[11−17] hydrogen/deuterium exchange,[18,19] electron capture dissociation,[20−22] and fast photochemical oxidation of proteins (FPOP)[23,24] have been combined with MS. In some cases, these hybrid techniques provide insight about low-abundance, and short-lived intermediates that is not accessible by more traditional approaches such as NMR, crystallography, or other spectroscopic methods.[24−27]

In the present work, we employ IMS−MS techniques to examine ubiquitin ions electrosprayed from different acidic water:methanol solutions. In ion mobility measurements, ions move through a buffer gas under the influence of a uniform electric field and are separated on the basis of differences in their shape and charge.[11] Structural information about the ion's overall geometry can be deduced by converting measured drift times into collision cross sections[28] and comparing these values with cross sections that are calculated for trial geometries generated by theoretical techniques such molecular dynamic simulations.[11,29−31] In the experiments described below, IMS−MS experiments are performed in a nested fashion, where mass spectra are recorded within individual drift windows across the IMS distribution,[32] making it possible to assess structures for multiple analytes and charge states in a single experiment. It is noteworthy that the extent to which the solvent-free macromolecule resembles its solution structure remains an active field of research.[16,22,33−38] The most stable structures of gas-phase ions are a result of the attractive intramolecular interactions and repulsive Coulombic forces.[39] The equilibrated gas-phase geometry of an ion can be substantially different from its structure in solution, for instance, high charge state ions are dominated by elongated structures with little similarity to the native form.[40] On the other hand, a number of studies provide evidence indicating that electrosprayed protein ions of low charge states, which are treated gently, can retain aspects of their solution-phase conformations, from elements of the secondary structure to the quaternary structure of a protein complex, on the time scale of milliseconds.[16,33−38]

Ubiquitin is a 76-amino acid polypeptide,[41,42] having one of the most conserved protein sequences; only three of its amino acids differ between the yeast and human sequences.[43−45] Analyses with NMR and circular dichroism (CD) spectroscopies indicate that ubiquitin remains the native (N) state in aqueous solutions at pHs as low as 2,[46] and that an addition of methanol to the acidic solution (pH ∼ 2) induces the formation of a partially folded structure, termed as the A

Received: September 30, 2013
Revised: February 4, 2014
Published: March 13, 2014

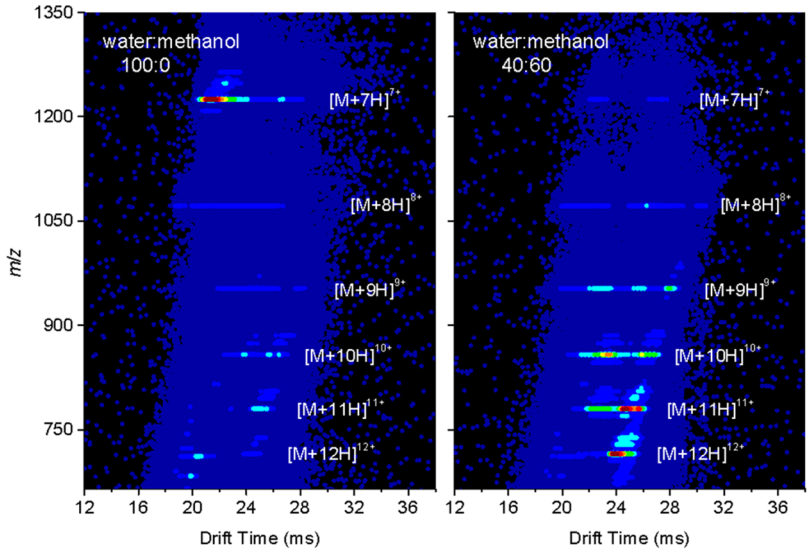

Figure 1. Two-dimensional drift time (m/z) contour plots for ubiquitin ions electrosprayed from an aqueous solution (left) and a solution of 40:60 water:methanol (right). The intensity of different features is shown with a false color scheme such that the most intense features are displayed in red and the least intense features are displayed in blue. Solution compositions (water:methanol) have been labeled. Both solutions are maintained at pH = 2. Ubiquitin ions of $[M + 7H]^{7+}$ to $[M + 12H]^{12+}$ are observed and each charge state has been labeled.

state.[47,48] The N form of ubiquitin is very compact and tightly hydrogen-bonded, which is composed of five β-strands that wrap around an α-helix and a 3_{10}-helix.[49] For the A state, NMR experiments performed in a 40:60 water:methanol solution suggest that it retains a majority of its native secondary structural elements in the N-terminal half, whereas the structure of the C-terminal half unfolds to a more elongated state with a high propensity of the helical structure.[47,48,50−55]

The present studies are closely related to a series of studies involving smaller peptides.[56,57] Remarkably, even relatively small peptides such as bradykinin (Arg-Pro-Pro-Gly-Phe-Ser-Pro-Phe-Arg)[56] and substance P (Arg-Pro-Lys-Pro-Gln-Gln-Phe-Phe-Gly-Leu-Met)[57] show evidence for many solution states. Those studies demonstrate that different solution states can generate dissimilar gas-phase conformers, such that it is possible to assess how many solution states are present in solution and to determine the populations of different solution states via gas-phase analysis.[56]

The present study is also closely related to our recent study of the cross section distributions for ubiquitin $[M + 8H]^{8+}$ ions.[58] In that work, ions were electrosprayed from 20 water:methanol solutions (100:0 to 5:95, pH = 2) and the IMS distributions were modeled with a set of Gaussian distributions.[58] The relative abundances for those Gaussian conformers varied as the solution compositions changed, which showed strong correlations to the solution N, A, and unfolded (U) states of ubiquitin.[58] Additionally, the Gaussian conformers for $[M + 7H]^{7+}$ ions were also reported.[59] In the current study, similar analyses are performed for $[M + 9H]^{9+}$ to $[M + 12H]^{12+}$ ions of ubiquitin produced from the same water:methanol solutions used previously, so that the entire distribution of ions formed during the electrospray ionization (ESI) process are examined. The main focus of this study was initially to identify and quantify these three solutions states (N, A, and U) of ubiquitin. However, this analysis suggests that we are actually sampling a total of five solution states under these conditions.

EXPERIMENTAL SECTION

Sample Preparation. As described previously,[58] solutions of bovine erythrocytes ubiquitin (≥98% purity, Sigma-Aldrich Co, St. Louis, MO) were prepared at a concentration of ~1 mg·mL^{-1} in water:methanol:formic acid mixtures (pH = 2). Twenty solution conditions were used with solution compositions ranging from 100:0 to 5:95 water:methanol (V:V), and the fraction of methanol was increased in increments of 5% for each solution.

IMS−MS Measurements. This work utilized a home-built IMS−MS instrument. IMS theory[28−30,60,61] and details of the instrumentation including the instrument used in these experiments[32,62−65] have been published elsewhere; only a brief summary is presented here. Ions were formed upon electrospraying ubiquitin solutions with a TriVersa NanoMate autosampler (Advion, Ithaca, NY). The Triversa Nanomate was operated with an electrospray voltage of 1.6 kV and a backing nitrogen gas pressure of 0.30 psi. The twenty ubiquitin solutions were electrosprayed and analyzed under the same instrument conditions. A continuous beam of protein ions was focused and accumulated in an hourglass ion funnel.[64] Periodically, packets of ions (150 μs wide) were gated into a 183 cm drift tube for mobility separation. The drift tube was filled with ~3.5 Torr of 300 K helium buffer gas and had a series of lenses and spacers to provide a uniform electric field which was ~10 V·cm^{-1} in this study. Ions drifted through the drift tube under the influence of the electric field and were separated on the basis of differences in collision cross sections. At the exit of the drift tube, ions were refocused by an ion funnel and extracted into the source of a time-of-flight (TOF) mass spectrometer where m/z values were measured. Drift times were collected in increments of 80 μs, which was the time required for recording a full mass spectrum to provide nested IMS−MS data sets as described previously.[32]

Determination of Collision Cross Sections. Collision cross sections (Ω) can be determined from the experimental drift times (t_D) according to eq 1[28]

dx.doi.org/10.1021/jp4097327 | J. Phys. Chem. B 2014, 118, 3498−3506

$$\Omega = \frac{(18\pi)^{1/2}}{16}\frac{ze}{(k_bT)^{1/2}}\left[\frac{1}{m_I}+\frac{1}{m_B}\right]^{1/2}\frac{t_DE}{L}\frac{760}{P}\frac{T}{273.2}\frac{1}{N} \quad (1)$$

where k_b is Boltzmann's constant, ze refers to the charge of the ion, and m_I and m_B are the masses of the ion and buffer gas, respectively. The variables E, L, and N correspond to the electric field, drift length and the neutral number density of the buffer gas at STP conditions, respectively. T and P correspond to buffer gas temperature and pressure, respectively. Collision cross sections determined from two measurements typically agree to within approximately 2%. Because of the incorporation of ion funnels in the split-field instruments, cross sections were not directly obtained from total drift times. Instead, the times that ions spent in the first drift region, which employed a highly uniform electric field, were measured and applied to the cross section determinations.

Data Analysis. As described previously,[58,59] Gaussian functions were employed to model the cross section distributions for ubiquitin ions of the +7 and +8 charge states. It was suggested that the observed experimental distribution consisted of a fixed number of conformation types, which could be represented by Gaussian distributions. Gaussian conformers that comprised the gas-phase distributions for the charge states of +9 to +12 were estimated. For each of the charge states, twenty IMS distributions generated from different water:-methanol solutions were treated as a data set and modeled with a minimum number of Gaussians. The form of a Gaussian distribution is given by eq 2

$$I = \frac{A}{\sigma\sqrt{2\pi}}e^{-(\Omega-\Omega_0)^2/2\sigma^2} \quad (2)$$

where I refers to the distribution intensity and the variable Ω represents the cross section. A, Ω_0, and σ correspond to the population, center, and width of the distribution of structures for the represented conformation type, respectively. The modeling was performed by using the Peak Analyzer tool in OriginPro 8.5.0 software (OriginLab Corporation, Northampton, MA). Peak centers and widths for the Gaussian distributions were optimized by altering the settings iteratively. While peak centers and widths were fixed between distributions of a single charge state, peak heights were modified to model the distributions. This process was repeated for each of the charge states from +9 to +12 to obtain the best Gaussian model.

RESULTS AND DISCUSSION

Nested $t_D(m/z)$ Plots for Ubiquitin Ions Formed by Electrospraying 100:0 and 40:60 Water:Methanol Solutions. Figure 1 shows the nested two-dimensional (2D) $t_D(m/z)$ plots for ubiquitin ions electrosprayed from two solutions, 100:0 and 40:60 water:methanol at pH = 2. The aqueous solution is known to favor the N-state ubiquitin, whereas A-state ubiquitin is dominant in the 40:60 water:-methanol solution.[46,47,53] The two plots display substantial variations in both charge state distributions and drift time distributions. The MS spectra shown here are similar to those published before.[66] For the aqueous solution, the main species generated is the $[M + 7H]^{7+}$ ion and only a small amount of ions with higher charge states (i.e., $[M + 8H]^{8+}$ to $[M + 12H]^{12+}$) are formed. In contrast, the 40:60 solution populates higher charge state ions (i.e., $[M + 10H]^{10+}$ to $[M + 12H]^{12+}$) and produces a trace amount of $[M + 7H]^{7+}$ ions. The shift to higher charge states for the A state is consistent with the fact that the A state is partially unfolded compared to the tightly folded native form.[53] The IMS−MS distributions also reveal differences in drift time distributions between ions originated from the N and A states. The distributions for $[M + 7H]^{7+}$ and $[M + 8H]^{8+}$ ions shift to more extended states when the solution composition is varied from 100:0 to 40:60 water:-methanol, which has been analyzed in detail in our previous work.[58,59] The $[M + 9H]^{9+}$ to $[M + 12H]^{12+}$ ions are mainly composed of partially folded and elongated conformations, the conformational variations of which between different solutions are described and discussed in more detail below.

Figure 2 shows plots of the normalized intensity for ubiquitin ions of different charge states as a function of methanol

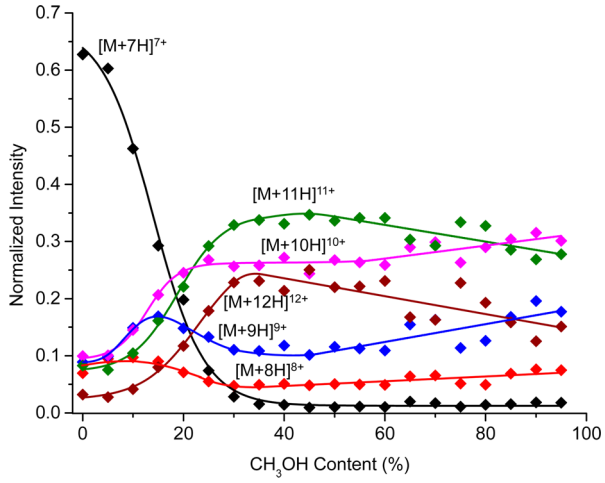

Figure 2. Normalized intensities for different charge states ($[M + 7H]^{7+}$ to $[M + 12H]^{12+}$) of ubiquitin ions as a function of methanol content. Charge states have been labeled for corresponding curves. The solid lines are drawn to guide the eye.

content. When electrosprayed from the 100:0 water:methanol solution, ubiquitin $[M + 7H]^{7+}$ ions dominate the distribution with an abundance of approximately 63%. The population for $[M + 7H]^{7+}$ ions drops dramatically with increased methanol content from 100:0 to 70:30 water: methanol solutions and remains around 1−2% with a further addition of methanol. The relative intensity for the $[M + 8H]^{8+}$ ions varies only slightly across all solution conditions with an average of 6 ± 2%, as reported before.[58] Specifically, the ion population decreases slightly when the fraction of methanol is raised from 0% to 30% and then increases marginally with further increments of methanol. $[M + 9H]^{9+}$ ions show a maximum intensity at the solution composition of 85:15 for solutions of 100:0 to 55:45 water:methanol, and a gradual increment in abundance from 55:45 to 5:95 solutions. The population of ubiquitin $[M + 10H]^{10+}$ ions increases sharply when the solution composition is changed from 100:0 to 80:20 water:methanol and then rises slowly with further additions of methanol. Moreover, $[M + 11H]^{11+}$ and $[M + 12H]^{12+}$ ions increase significantly in population with the change of solution compositions from 100:0 to 65:35 water:methanol, whereas they become less abundant with a further increase in methanol. Figure 2 clearly demonstrates that increasing the methanol content in solution shifts the charge state distribution of ubiquitin toward higher charge states (i.e., +10 to +12) from 100:0 to 60:40

dx.doi.org/10.1021/jp4097327 | J. Phys. Chem. B 2014, 118, 3498−3506

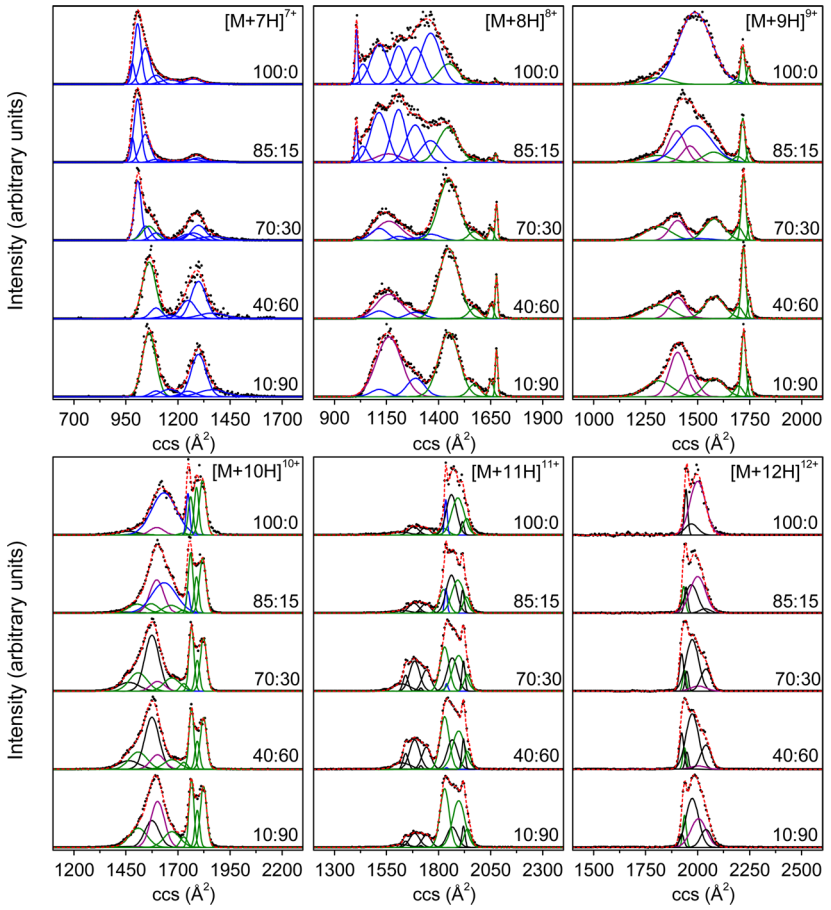

Figure 3. Collision cross section (ccs) distributions (solid circles) for different charge states ($[M + 7H]^{7+}$ to $[M + 12H]^{12+}$) of ubiquitin ions from five water:methanol solutions. Solution compositions (water:methanol) have been labeled for each distribution. The Gaussian functions employed to model the experimental distributions are plotted as solid lines and the sum of Gaussian functions is drawn as a red dashed line. Gaussian functions representing conformation types that are assigned to the N, A, and A′ states of ubiquitin are plotted in blue, green, and black, respectively (see text for more details). The U and B conformers are plotted in purple. Part of the distributions for $[M + 7H]^{7+}$ and $[M + 8H]^{8+}$ ions are from refs 58 and 59.

water:methanol solutions, whereas ions populate more intermediate charge states (i.e., +9 and +10) from 60:40 to 5:95 solutions. The observed transition in charge state distributions indicates that methanol induces structural transitions for ubiquitin.

Collision Cross Section Distributions (from IMS Data) for Ubiquitin Ions from Different Water:Methanol Solutions. Collision cross section distributions for ubiquitin $[M + 7H]^{7+}$ to $[M + 12H]^{12+}$ ions electrosprayed from five water:methanol solutions, selected as representatives of the twenty distributions, are shown in Figure 3. The main features observed for ubiquitin ions generated from the high methanol solutions are consistent with results published before,[67] with some subtle differences. The cross sections for elongated structures are in good agreement with previous results.[67] The differences in distributions probably arise from differences in solution (i.e., the pH of the solutions) and instrument conditions.

The distributions for $[M + 7H]^{7+}$ and $[M + 8H]^{8+}$ ions have been described in the previous work.[58,59] For the aqueous solution, the spectrum obtained for ubiquitin $[M + 7H]^{7+}$ ions is dominated by a peak centered at ~1010 Å^2 corresponding to compact structures. A small peak is also observed at ~1280 Å^2, which is composed of partially folded states. We note that the compact structures for $[M + 7H]^{7+}$ ions have similar cross sections to that of the compact conformations of $[M + 8H]^{8+}$ ions (1020 Å^2). These compact states are slightly contracted in size compared to the N state of ubiquitin; the cross section calculated from the coordinates of the crystal structure is about 1090 Å^2. The $[M + 7H]^{7+}$ ions display a broader distribution of compact states than that for the $[M + 8H]^{8+}$ ions which shows a very sharp peak in the region of compact structures. This indicates that $[M + 7H]^{7+}$ ions have a broader range of compact configurations that are accessible in the folding funnel under current experimental conditions due to lower Coulombic repulsions. As the solution composition reaches 70:30 water:-methanol, a shoulder centered at ~1060 Å^2 emerges at the right side of the 1010 Å^2 peak. The partially folded structures shift to slightly larger cross sections around 1300 Å^2 with an increased intensity compared to that of the aqueous solution. With higher methanol content, the 1060 Å^2 peak dominates the compact structure distribution and the 1300 Å^2 peak becomes more intense. As mentioned before, ubiquitin $[M + 8H]^{8+}$ ions favor a sharp feature at 1020 Å^2 and a broad distribution of structures ranging from approximately 1040 to 1620 Å^2 for the aqueous solution.[58] Ubiquitin ions electrosprayed from high methanol solutions form two broad distributions centered at ~1150 and ~1450 Å^2 and two sharp peaks of extended states at 1650 and 1680 Å^2. For the IMS profiles of ubiquitin $[M + 9H]^{9+}$ ions, the aqueous solution favors a broad distribution of structures

dx.doi.org/10.1021/jp4097327 | J. Phys. Chem. B 2014, 118, 3498−3506

Table 1. Values of Peak Centers Ω_0 (Å^2) and Standard Deviations σ (Å^2) for Gaussian Functions Employed To Represent the Conformation Types of Ubiquitin Ions ($[M + 7H]^{7+}$ to $[M + 12H]^{12+}$)

$[M+7H]^{7+}$			$[M+8H]^{8+}$			$[M+9H]^{9+}$			$[M+10H]^{10+}$			$[M+11H]^{11+}$			$[M+12H]^{12+}$		
Ω_0 (σ)[†]	SS*	#	Ω_0 (σ)	SS	#	Ω_0 (σ)	SS	#	Ω_0 (σ)	SS	#	Ω_0 (σ)	SS	#	Ω_0 (σ)	SS	#
980 (11)	N1	●	1020 (6)	N1	△	1310 (64)	A1	○	1460 (49)	A′1	●	1620 (41)	A′1	■	1920 (11)	A′1	●
1010 (17)	N2	■	1040 (25)	N2	■	1400 (39)	U1	■	1510 (42)	A1	■	1640 (12)	A′2	●	1940 (8)	A	■
1040 (25)	N3	△	1120 (41)	N3	▲	1400 (39)	B1	■	1570 (34)	A′2	▲	1680 (25)	A′3	▲	1950 (8)	A′2	△
1060 (32)	A	■	1160 (60)	U	■	1470 (36)	U2	▲	1600 (33)	U	■	1710 (7)	A′4	◘	1970 (31)	A′3	▲
1100 (28)	N4	◘	1160 (60)	B	■	1470 (36)	B2	▲	1600 (33)	B	■	1740 (22)	A′5	○	2000 (37)	U	●
1160 (42)	N5	○	1210 (34)	N4	●	1490 (80)	N	■	1640 (59)	N1	●	1830 (22)	A1	●	2000 (37)	B	●
1250 (36)	N6	▲	1290 (42)	N5	◘	1580 (48)	A2	■	1670 (39)	A2	◘	1840 (6)	N	○	2040 (25)	A′4	○
1280 (38)	N7	×	1360 (47)	N6	○	1700 (20)	A3	◘	1730 (17)	A3	○	1860 (25)	A′6	△			
1300 (36)	N8	⊕	1450 (49)	A1	■	1720 (11)	A4	●	1750 (8)	N2	■	1900 (30)	A2	△			
1370 (64)	N9	⁂	1570 (28)	A2	△	1750 (8)	A5	▲	1760 (12)	A4	△	1920 (8)	A′7	×			
			1650 (11)	A3	×				1790 (11)	A5	×	1940 (16)	A3	⊕			
			1680 (6)	A4	⊕				1820 (16)	A6	⊕						

[†]Values for $[M + 7H]^{7+}$ and $[M + 8H]^{8+}$ ions have been reported in refs 58 and 59. *Solution states (N, A, A′, U, and B) assigned to the respective gas-phase conformation types. #Symbols used for respective Gaussian functions plotted in Figure 4.

ranging in size from ~1140 to ~1670 Å^2 centered at ~1490 Å^2 and a relatively sharp peak at ~1720 Å^2. Compared to $[M + 7H]^{7+}$ and $[M + 8H]^{8+}$ ions, $[M + 9H]^{9+}$ ions produce a distribution of structures that are more elongated, which is attributed to higher Coulombic repulsions between charges. The elongated states at ~1720 Å^2 exist across all solution conditions with increased intensities at higher methanol content. On the other hand, the broad distribution shifts to smaller cross sections centered at ~1430 Å^2 and also evolves a shoulder at ~1520 Å^2 for the 85:15 water:methanol solution. When the solution composition reaches 70:30, the broad distribution shown in the aqueous solution splits into two peaks at ~1400 and ~1580 Å^2, the former of which becomes more populated for the 10:90 water:methanol solution.

Compared with distributions for the low charge states of ubiquitin ions, variations in the cross section distributions observed for the high charge states (i.e., +10 to +12) between different water:methanol solutions are more subtle. This is because the Coulombic repulsion becomes the dominant factor in dictating the anhydrous conformations for ubiquitin ions of high charge states, whereas the initial solution structures play a more important role for the low charge state ions. Ubiquitin $[M + 10H]^{10+}$ ions generate a distribution with a broad peak extending from ~1350 to ~1720 Å^2, which is centered at ~1630 Å^2, as well as two partially resolved elongated features at ~1750 and ~1800 Å^2 under the 100:0 water:methanol solution condition. The overall shape of the distribution for ions produced from the 70:30 solution is similar to that generated from the aqueous solution; the broad peak shifts to smaller cross sections with a maximum at ~1580 Å^2, whereas the two elongated features shift to ~1760 and ~1820 Å^2. There are no significant changes for distributions of ions formed from even higher methanol solutions. Distributions for ubiquitin $[M + 11H]^{11+}$ ions show a population of unresolved conformers, with cross sections ranging from ~1550 to ~1780 Å^2 (corresponding to elongated forms). Additionally, more intense features are observed for even larger cross section ions from ~1780 to ~2000 Å^2 and the distributions display two maxima at 1840 and 1920 Å^2 across all solution conditions. Their relative intensities vary as the methanol content changes. More specifically, the distribution for structures with smaller cross sections is of very low intensity for the 100:0 water:methanol solution but becomes more abundant with an increase in methanol content from 100:0 to 40:60 solutions. When the solution composition reaches 10:90 water:methanol, this population decreases. The $[M + 12H]^{12+}$ distribution is dominated by two partially resolved features at ~1940 and ~2000 Å^2 for the aqueous solution. For solutions of 70:30 and 40:60 water:methanol, the peak at ~1940 Å^2 becomes more intense with two shoulders at ~1980 and ~2040 Å^2, whereas the population of ions at ~1980 Å^2 is more intense for the 10:90 solution.

Modeling Cross Section Distributions with Gaussian Functions. To make additional progress in characterizing the solution populations of this system, we have modeled all of the cross section distributions with Gaussian functions. This approach is similar to the approach we developed for assessing ubiquitin $[M + 8H]^{8+}$ ions.[58] The approach allows us to quantify small differences in population that arise with subtle changes in solution composition. Here, we examine the +9 to +12 charge states. We consider that the gradual changes in IMS distributions between different water:methanol solutions arise from variations in populations of a fixed number of gas-phase conformers. Those conformers comprise the experimental distributions across all solutions. In the modeling, a set of Gaussian functions are employed to represent these gas-phase conformers for each charge state, with only peak heights varying between different distributions. The Gaussian distributions that we determined best to model the IMS distributions are displayed in Figure 3. The sums of these Gaussians are also shown in Figure 3, which demonstrates a good fit to the experimental data. The modeling results show that ten, eleven, eight, eleven, eleven, and six Gaussian functions are necessary to model the distributions for +7, +8, +9, +10, +11, and +12 charge states, respectively. Peak centers and widths of the

dx.doi.org/10.1021/jp4097327 | J. Phys. Chem. B 2014, 118, 3498−3506

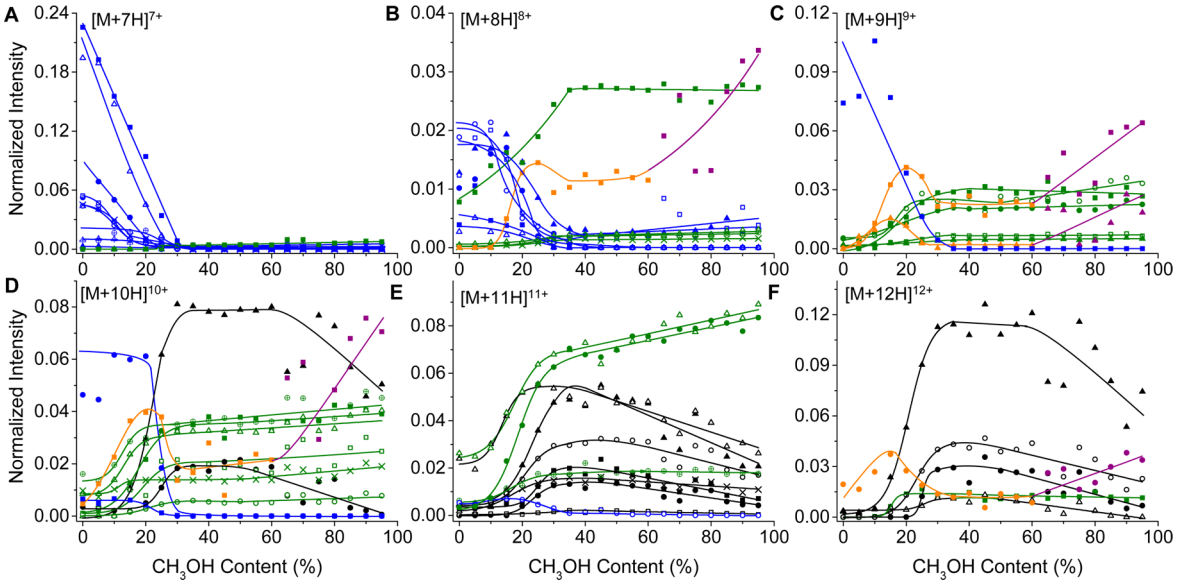

Figure 4. Normalized intensity for different Gaussian conformers as a function of solvent methanol content. (A)−(F) show the results for charge states of $[M + 7H]^{7+}$ to $[M + 12H]^{12+}$, respectively. Conformation types that are assigned to the N, A, A′, U, and B of ubiquitin are plotted in blue, green, black, purple, and orange, respectively (see text for more details), and the respective symbols for different conformers are listed in Table 1. The solid lines are drawn to guide the eye.

employed Gaussian functions are summarized in Table 1. The analysis and interpretation of these Gaussians is given below.

Correlating Ubiquitin Gas-Phase Conformation Types to Solution States. It is worthwhile to plot the relative abundances of the determined gas-phase conformers at different methanol content, such that they can be correlated to the solution states of ubiquitin. Parts A−F of Figure 4 show the fraction of different gas-phase conformers over the total ion population for ubiquitin $[M + 7H]^{7+}$ to $[M + 12H]^{12+}$ ions, respectively. In this analysis, we assume those gas-phase conformers (in this case, the individual Gaussian distributions that are used to model the set of IMS distributions for all charge states) that show similar variations in the relative abundances as the methanol content changes must arise from the same solution state. On the other hand, Gaussian intensities that vary differently with solution composition are assumed to arise from different solution structures. Our previous study[58] described the relative intensities of ubiquitin $[M + 8H]^{8+}$ conformers over the total $[M + 8H]^{8+}$ ion population. Because the population for $[M + 8H]^{8+}$ ions is relatively constant across all solutions with an average of 6 ± 2% over the total ion population, the abundance profiles for $[M + 8H]^{8+}$ conformers normalized to the total ion population have a similar appearance to profiles for conformers normalized to the total $[M + 8H]^{8+}$ ion population with subtle variations. As described previously,[58] gas-phase conformation types that are suggested to arise from the solution N state decrease in intensity as the methanol content increases and are almost completely absent for solution compositions beyond 65:35 water:methanol; those generated from the solution A state are abundant for solutions from 70:30 to 5:95 water:methanol; and that for the U state displays a different abundance profile from N and A states, which shows a substantial increase when the solution composition is changed from 40:60 to 5:95 water:methanol.

Conformers (plotted in blue, Figure 4) with population profiles similar in appearance to the $[M + 8H]^{8+}$ N-state conformers are also observed for other charge state ions, predominantly at low charge states. Our result is similar to Wyttenbach and Bowers' work[38] that the compact conformations of the +7 and +8 charge states arise from the N-state ubiquitin. In addition, unfolding of the solution N structure also occurs during the ESI process, such that some of the N-state conformers are observed as partially folded and elongated states in the gas phase. All except the Ω = 1060 ± 32 Å^2 conformer for $[M + 7H]^{7+}$ ions decay significantly as the methanol content increases, which is consistent with what is expected for the N state. For the charge state of +8, as mentioned before,[58] six conformers are identified corresponding to the N structure. Only one or two gas-phase conformers are produced from the N state for $[M + 9H]^{9+}$ (Ω = 1490 ± 80 Å^2), $[M + 10H]^{10+}$ (Ω = 1640 ± 59 and Ω = 1750 ± 8 Å^2), and $[M + 11H]^{11+}$ (Ω = 1840 ± 6 Å^2) ions; none of the $[M + 12H]^{12+}$ ions is generated from the N state. The assigned solution states for different gas-phase conformers are also listed in Table1.

Conformers of the $[M + 8H]^{8+}$ ions (i.e., the Ω = 1450 ± 49 Å^2, Ω = 1570 ± 28 Å^2, Ω = 1650 ± 11 Å^2, and Ω = 1680 ± 6 Å^2 peaks) that had been assigned to the A-state ubiquitin in the previous study[58] become considerably more intense from 100:0 to 70:30 water:methanol solutions and remain relatively constant in population with a further increase in the methanol percentage. This type of structure (plotted in green, Figure 4) is also observed for other charge state ions, primarily for $[M + 9H]^{9+}$ to $[M + 11H]^{11+}$ ions. As displayed in Figure 4, the gas-phase conformers for ubiquitin suggest that there are at least two additional types of populations in addition to those expected for the N and A states, indicating the presence of additional ubiquitin structures in water:methanol solutions. In the following sections, we describe two new states of ubiquitin that have not been detected before.

Evidence for a New A-like State (the A′ State). During the course of this analysis, we have found that some of the Gaussian distributions that are required to model the experimental data do not follow any of the changes in abundance that are associated with peaks that are used to model the known N, A, and U states. However, these Gaussians do behave similarly when compared to each other. Thus, as

dx.doi.org/10.1021/jp4097327 | J. Phys. Chem. B 2014, 118, 3498−3506

described below, we propose that these Gaussians are capturing evidence for new conformers in solution that have not been reported previously.

Figure 4 indicates the existence of a type of conformer (plotted in black), such as the $\Omega = 1570 \pm 34$ Å^2 peak for the +10 charge state, the $\Omega = 1680 \pm 25$ Å^2 peak for the +11 charge state, and the $\Omega = 1970 \pm 31$ Å^2 peak for the +12 charge state (as listed in Table 1), that is very similar in its abundance profile to the A-state conformers. The relative intensities of this type of conformer increase substantially from 100:0 to 70:30 water:methanol solutions, similar to the case for the A state. However, the population of these structures drops noticeably with a further increase in methanol for solutions from 40:60 to 10:90 water:methanol, distinguishing them from the A-state conformers. Considering that this type of gas-phase conformer has behaviors from 100:0 to 40:60 water:methanol solutions very similar to those of the A state, it is very likely generated from a solution state that is closely related to the A state. We term this type of conformer the A′ state. The A′-state ubiquitin primarily generates high charge state ions (+9 to +12) during the ESI process (Table 1).

Evidence for the Existence of a New Low-Abundance State of Ubiquitin (the B State). The fourth type of abundance profiles (plotted in orange/purple, Figure 4) shows a more complicated shape. The relative intensity increases from 100:0 to ∼80:20 water:methanol solutions but decreases from ∼80:20 to ∼70:30 solutions. Then the population of this conformer type keeps fairly constant for solutions from 70:30 to ∼40:60 water:methanol, followed by a substantial rise with further increased percentages of methanol. This type of conformer is observed for the $[M + 8H]^{8+}$ ($\Omega = 1160 \pm 60$ Å^2, which was defined as the U state previously[58]), $[M + 9H]^{9+}$ ($\Omega = 1400 \pm 39$ and $\Omega = 1470 \pm 36$ Å^2), $[M + 10H]^{10+}$ ($\Omega = 1600 \pm 33$ Å^2), and $[M + 12H]^{12+}$ ($\Omega = 2000 \pm 37$ Å^2) ions, as listed in Table 1.

The shape of the fourth type of abundance profiles suggests that these gas-phase conformers are generated from two solution states. The first state begins to populate from the aqueous solution and becomes more intense as the methanol content increases. It reaches its maximum intensity at ∼80:20 water:methanol and then the intensity of this state drops with a further increase in methanol content. The population of this state remains relatively constant from 70:30 to 40:60 water:methanol solutions. The second state is favored in high methanol solutions from 40:60 to 5:95 water:methanol. The behavior of the second solution state is consistent with that expected for the U state. However, the first state appears to be generated from a new solution state that has not been distinguished previously. We refer to this new state as the B state of ubiquitin. It is interesting to note that the U and B states of ubiquitin produce gas-phase conformers with similar cross sections.

Quantifying Solution States in Different Water:-Methanol Solutions. By summing the relative intensities of ubiquitin gas-phase conformers arising from the same solution state (N, A, A′, U, and B), the populations for each of the solution states can be quantified. Figure 5 plots the relative abundances for N, A, A′, U, and B states of ubiquitin in different water:methanol solutions which are maintained at pH = 2. As displayed, the 100:0 water:methanol solution favors the N-state ubiquitin, which contributes approximately 80% of the total population. Thus, even though the N state dominates the population, small amounts of other ubiquitin species exist in an

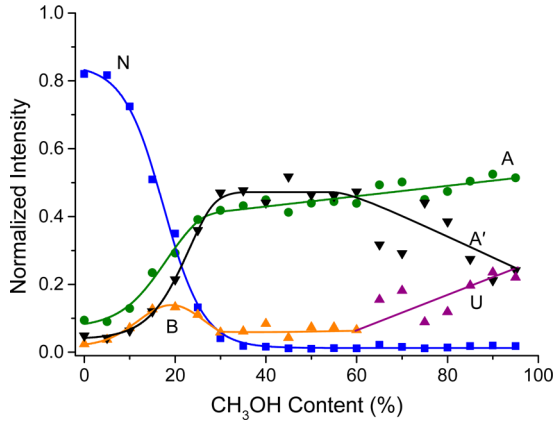

Figure 5. Normalized intensities for different solution states (N, A, A′, U, and B) of ubiquitin as a function of methanol content. Solutions states have been labeled near corresponding curves. The solid lines are drawn to guide the eye.

aqueous solution of low pH. With increased percentages of methanol in solution, the N-state ubiquitin is less populated and other non-native A, A′, U, and B states are favored. When the solution composition reaches 80:20 water:methanol, N-, A-, A′-, and B-state ubiquitin coexist at equilibrium in the solution. These different solution structures can be trapped and evolve into dissimilar gas-phase conformers upon dehydration. The populations for the A and A′ states of ubiquitin keep increasing with a further increase in methanol, whereas the B-state ubiquitin (∼10%) becomes less populated. On this basis, we speculate that the structure of the B state may have N and A character. From 70:30 to 40:60 solutions, the A- and A′-state ubiquitins are highly favored and only a very small amount of N (∼1%) and B (∼6%) states exist. Across this range of solution compositions, different ubiquitin states remain relatively constant in population. In solutions with even higher methanol content, the U-state ubiquitin becomes populated, whereas the A′ state decays noticeably. From this behavior we speculate that the A′-state ubiquitin has a structure related to both the A and U states.

SUMMARY AND CONCLUSIONS

Ubiquitin ions electrosprayed from 20 water:methanol solutions (pH = 2) with solution compositions ranging from 100:0 to 5:95 have been measured by IMS−MS. Ubiquitin $[M + 7H]^{7+}$ to $[M + 12H]^{12+}$ ions are formed across all solutions. The aqueous solution primarily generates $[M + 7H]^{7+}$ ions, whereas the high charge state ions (i.e., $[M + 10H]^{10+}$ to $[M + 12H]^{12+}$) are favored in solutions with high methanol content. The obtained cross section distributions for each charge state have been modeled by a set of Gaussian distributions with the aim of determining possible gas-phase conformers. The relative abundances for different conformation types over the total ion population have been measured and plotted as of a function of methanol content. Based on their variations in population with changes in methanol content, the gas-phase conformers have been assigned to N, A, A′, U, and B states of ubiquitin. The N state is highly favored in the aqueous solution with a relative intensity of ∼80%, whereas A and A′ states dominate the population for solutions ranging from 70:30 to 40:60 water:methanol wherein they contribute ∼93% of the total population. At the solution composition of 5:95 water:-methanol, the A state is still populated with a relative

dx.doi.org/10.1021/jp4097327 | J. Phys. Chem. B 2014, 118, 3498−3506

abundance of ~50% and a significant amount of U and A′ structures are also observed with a relative intensity of ~20% and 25%, respectively. This work presents the first evidence for the existence of a new and low-abundance state of ubiquitin, the B state, that is populated from 100:0 to 70:30 water:methanol solutions with a maximum intensity (~10%) observed at 80:20 water:methanol. Analysis of the population profiles for these solution states at different methanol content leads us to speculate that B-state ubiquitin may be closely related to the N and A states and the A′ state has similarities with the A and U states.

The observation of new solution states of ubiquitin by use of gas-phase techniques suggests that it is possible to effectively freeze out states that arise from solution and to distinguish between them based on their gas-phase structures. Such an analysis should be especially sensitive to low-abundance compounds (e.g., the B state) that are not perceivable by conventional structural determination methods.

AUTHOR INFORMATION

Corresponding Author

*D. E. Clemmer: e-mail, clemmer@indiana.edu.

Notes

The authors declare no competing financial interest.

ACKNOWLEDGMENTS

We gratefully acknowledge partial funding of this work from grants that support instrumentation development. These include grants from the NIH (1RC1GM090797-02) and funds from the Indiana University METACyt initiative that is funded by a grant from the Lilly Endowment.

REFERENCES

(1) Ishima, R.; Torchia, D. A. Protein Dynamics from NMR. *Nat. Struct. Biol.* **2000**, *7*, 740−743.

(2) Bahar, I.; Lezon, T. R.; Yang, L.-W.; Eyal, E. Global Dynamics of Proteins: Bridging Between Structure and Function. *Annu. Rev. Biophys.* **2010**, *39*, 23−42.

(3) Chowdhury, S. K.; Katta, V.; Chait, B. T. An Electrospray-Ionization Mass Spectrometer with New Features. *Rapid Commun. Mass Spectrom.* **1990**, *4*, 81−87.

(4) Suckau, D.; Shi, Y.; Beu, S. C.; Senko, M. W.; Quinn, J. P.; Wampler, F. M.; McLafferty, F. W. Coexisting Stable Conformations of Gaseous Protein Ions. *Proc. Natl. Acad. Sci. U. S. A.* **1993**, *90*, 790−793.

(5) Konermann, L.; Rosell, F. I.; Mauk, A. G.; Douglas, D. J. Acid-Induced Denaturation of Myoglobin Studied by Time-Resolved Electrospray Ionization Mass Spectrometry. *Biochemistry* **1997**, *36*, 6448−6454.

(6) Frimpong, A. K.; Abzalimov, R. R.; Eyles, S. J.; Kaltashov, I. A. Gas-Phase Interference-Free Analysis of Protein Ion Charge-State Distributions: Detection of Small-Scale Conformational Transitions Accompanying Pepsin Inactivation. *Anal. Chem.* **2007**, *79*, 4154−4161.

(7) Kaltashov, I. A.; Abzalimov, R. R. Do Ionic Charges in ESI MS Provide Useful Information on Macromolecular Structure? *J. Am. Soc. Mass Spectrom.* **2008**, *19*, 1239−1246.

(8) Konermann, L.; Ahadi, E.; Rodriguez, A. D.; Vahidi, S. Unraveling the Mechanism of Electrospray Ionization. *Anal. Chem.* **2013**, *85*, 2−9.

(9) Stahl-Zeng, J.; Lange, V.; Ossola, R.; Eckhardt, K.; Krek, W.; Aebersold, R.; Domon, B. High Sensitivity Detection of Plasma Proteins by Multiple Reaction Monitoring of N-Glycosites. *Mol. Cell. Proteomics* **2007**, *6*, 1809−1817.

(10) Heck, A. J. R. Native Mass Spectrometry: a Bridge Between Interactomics and Structural Biology. *Nat. Methods* **2008**, *5*, 927−933.

(11) Clemmer, D. E.; Jarrold, M. F. Ion Mobility Measurements and their Applications to Clusters and Biomolecules. *J. Mass Spectrom.* **1997**, *32*, 577−592.

(12) Clemmer, D. E.; Hudgins, R. R.; Jarrold, M. F. Naked Protein Conformations: Cytochrome *c* in the Gas Phase. *J. Am. Chem. Soc.* **1995**, *117*, 10141−10142.

(13) Bohrer, B. C.; Merenbloom, S. I.; Koeniger, S. L.; Hilderbrand, A. E.; Clemmer, D. E. Biomolecule Analysis by Ion Mobility Spectrometry. *Annu. Rev. Anal. Chem.* **2008**, *1*, 293−327.

(14) Liu, X.; Valentine, S. J.; Plasencia, M. D.; Trimpin, S.; Naylor, S.; Clemmer, D. E. Mapping the Human Plasma Proteome by SCX−LC−IMS−MS. *J. Am. Soc. Mass Spectrom.* **2007**, *18*, 1249−1264.

(15) Gaye, M. M.; Valentine, S. J.; Hu, Y.; Mirjankar, N.; Hammoud, Z. T.; Mechref, Y.; Lavine, B. K.; Clemmer, D. E. Ion Mobility-Mass Spectrometry Analysis of Serum N-Linked Glycans from Esophageal Adenocarcinoma Phenotypes. *J. Proteome. Res.* **2012**, *11*, 6102−6110.

(16) Ruotolo, B. T.; Giles, K.; Campuzano, I.; Sandercock, A. M.; Bateman, R. H.; Robinson, C. V. Evidence for Macromolecular Protein Rings in the Absence of Bulk Water. *Science* **2005**, *310*, 1658−1661.

(17) Uetrecht, C.; Barbu, I. M.; Shoemaker, G. K.; van Duijn, E.; Heck, A. J. R. Interrogating Viral Capsid Assembly with Ion Mobility-Mass Spectrometry. *Nat. Chem.* **2011**, *3*, 126−132.

(18) Zhang, Z.; Smith, D. L. Determination of Amide Hydrogen Exchange by Mass Spectrometry: a New Tool for Protein Structure Elucidation. *Protein Sci.* **1993**, *2*, 522−531.

(19) Konermann, L.; Pan, J.; Liu, Y.-H. Hydrogen Exchange Mass Spectrometry for Studying Protein Structure and Dynamics. *Chem. Soc. Rev.* **2011**, *40*, 1224−1234.

(20) Breuker, K.; Oh, H. B.; Horn, D. M.; Cerda, B. A.; McLafferty, F. W. Detailed Unfolding and Folding of Gaseous Ubiquitin Ions Characterized by Electron Capture Dissociation. *J. Am. Chem. Soc.* **2002**, *124*, 6407−6420.

(21) Robinson, E. W.; Leib, R. D.; Williams, E. R. the Role of Conformation on Electron Capture Dissociation of Ubiquitin. *J. Am. Soc. Mass Spectrom.* **2006**, *17*, 1469−1479.

(22) Skinner, O. S.; McLafferty, F. W.; Breuker, K. How Ubiquitin Unfolds after Transfer into the Gas Phase. *J. Am. Soc. Mass Spectrom.* **2012**, *23*, 1011−1014.

(23) Gau, B. C.; Sharp, J. S.; Rempel, D. L.; Gross, M. L. Fast Photochemical Oxidation of Protein Footprints Faster than Protein Unfolding. *Anal. Chem.* **2009**, *81*, 6563−6571.

(24) Chen, J.; Rempel, D. L.; Gau, B. C.; Gross, M. L. Fast Photochemical Oxidation of Proteins and Mass Spectrometry Follow Submillisecond Protein Folding at the Amino-Acid Level. *J. Am. Soc. Chem.* **2012**, *134*, 18724−18731.

(25) Bleiholder, C.; Dupuis, N. F.; Wyttenbach, T.; Bowers, M. T. Ion Mobility−Mass Spectrometry Reveals a Conformational Conversion from Random Assembly to β-Sheet in Amyloid Fibril Formation. *Nat. Chem.* **2011**, *2*, 172−177.

(26) Wilson, D. J.; Rafferty, S. P.; Konermann, L. Kinetic Unfolding Mechanism of the Inducible Nitric Oxide Synthase Oxygenase Domain Determined by Time-Resolved Electrospray Mass Spectrometry. *Biochemistry* **2005**, *44*, 2276−2283.

(27) Pan, J.; Han, J.; Borchers, C. H.; Konermann, L. Characterizing Short-Lived Protein Folding Intermediates by Top-Down Hydrogen Exchange Mass Spectrometry. *Anal. Chem.* **2010**, *82*, 8591−8597.

(28) Mason, E. A.; McDaniel, E. W. *Transport Properties of Ions in Gases*; Wiley: New York, 1988.

(29) Mesleh, M. F.; Hunter, J. M.; Shvartsburg, A. A.; Schatz, G. C.; Jarrold, M. F. Structural Information from Ion Mobility Measurements: Effects of the Long-Range Potential. *J. Phys. Chem.* **1996**, *100*, 16082−16086.

(30) Wyttenbach, T.; von Helden, G.; Batka, J. J.; Carlat, D.; Bowers, M. T. Effect of the Long-Range Potential on Ion Mobility Measurements. *J. Am. Soc. Mass Spectrom.* **1997**, *8*, 275−282.

(31) Politis, A.; Park, A. Y.; Hyung, S.-J.; Barsky, D.; Ruotolo, B. T.; Robinson, C. V. Integrating Ion Mobility Mass Spectrometry with Molecular Modeling to Determine the Architecture of Multiprotein Complexes. *PLoS ONE* **2010**, *5*, e12080.

(32) Hoaglund, C. S.; Valentine, S. J.; Sporleder, C. R.; Reilly, J. P.; Clemmer, D. E. Three-Dimensional Ion Mobility/TOFMS Analysis of Electrosprayed Biomolecules. *Anal. Chem.* **1998**, *70*, 2236−2242.
(33) Loo, J. A. Studying Noncovalent Protein Complexes by Electrospray Ionization Mass Spectrometry. *Mass Spectrom. Rev.* **1997**, *16*, 1−23.
(34) Loo, J. A.; He, J. X.; Cody, W. L. Higher Order Structure in the Gas Phase Reflects Solution Structure. *J. Am. Chem. Soc.* **1998**, *120*, 4542−4543.
(35) Ruotolo, B. T.; Robinson, C. V. Aspects of Native Proteins are Retained in Vacuum. *Curr. Opin. Chem. Biol.* **2006**, *10*, 402−408.
(36) Koeniger, S. L.; Merenbloom, S. I.; Sevugarajan, S.; Clemmer, D. E. Transfer of Structural Elements from Compact to Extended States in Unsolvated Ubiquitin. *J. Am. Chem. Soc.* **2006**, *128*, 11713−11719.
(37) Liu, L.; Bagal, D.; Kitova, E. N.; Schnier, P. D.; Klassen, J. S. Hydrophobic Protein-Ligand Interactions Preserved in the Gas Phase. *J. Am. Chem. Soc.* **2009**, *131*, 15980−15981.
(38) Wyttenbach, T.; Bowers, M. T. Structural Stability from Solution to the Gas Phase: Native Solution Structure of Ubiquitin Survives Analysis in a Solvent-Free Ion Mobility-Mass Spectrometry Environment. *J. Phys. Chem. B* **2011**, *115*, 12266−12275.
(39) Valentine, S. J.; Anderson, J. G.; Ellington, A. D.; Clemmer, D. E. Disulfide-Intact and -Reduced Lysozyme in the Gas Phase: Conformations and Pathways of Folding and Unfolding. *J. Phys. Chem. B* **1997**, *101*, 3891−3900.
(40) Valentine, S. J.; Counterman, A. E.; Clemmer, D. E. Conformer-Dependent Proton-Transfer Reactions of Ubiquitin Ions. *J. Am. Soc. Mass. Spectrom.* **1997**, *8*, 954−961.
(41) Goldstein, G.; Scheid, M.; Hammerling, U.; Boyse, E. A.; Schlesinger, D. H.; Niall, H. D. Isolation of a Polypeptide that Has Lymphocyte-Differentiating Properties and is Probably Represented Universally in Living Cells. *Proc. Natl. Acad. Sci. U. S. A.* **1975**, *72*, 11−15.
(42) Rechsteiner, M. *Ubiquitin*; Plenum Press: New York, 1988.
(43) Wilkinson, K. D.; Cox, M. J.; O'Connor, L. B.; Shapira, R. Structure and Activities of a Variant Ubiquitin Sequence from Bakers' Yeast. *Biochemistry* **1986**, *25*, 4999−5004.
(44) Vijay-Kumar, S.; Bugg, C. E.; Wilkinson, K. D.; Vierstra, R. D.; Hatfield, P. M.; Cook, W. J. Comparison of the Three-Dimensional Structures of Human, Yeast, and Oat Ubiquitin. *J. Biol. Chem.* **1987**, *262*, 6396−6399.
(45) Jentsch, S. The Ubiquitin-Conjugation System. *Annu. Rev. Genet.* **1992**, *26*, 179−207.
(46) Lenkinski, R. E.; Chen, D. M.; Glickson, J. D.; Goldstein, G. Nuclear Magnetic Resonance Studies of Denaturation of Ubiquitin. *Biochim. Biophys. Acta* **1977**, *494*, 126−130.
(47) Wilkinson, K. D.; Mayer, A. N. Alcohol-Induced Conformational Changes of Ubiquitin. *Arch. Biochem. Biophys.* **1986**, *250*, 390−399.
(48) Harding, M. M.; Williams, D. H.; Woolfson, D. N. Characterization of a Partially Denatured State of a Protein by Two-Dimensional NMR: Reduction of the Hydrophobic Interactions in Ubiquitin. *Biochemistry* **1991**, *30*, 3120−3128.
(49) Vijay-Kumar, S.; Bugg, C. E.; Cook, W. J. Structure of Ubiquitin Refined at 1.8 Å Resolution. *J. Mol. Biol.* **1987**, *194*, 531−544.
(50) Pan, Y.; Briggs, M. S. Hydrogen Exchange in Native and Alcohol Forms of Ubiquitin. *Biochemistry* **1992**, *31*, 11405−11412.
(51) Stockman, B. J.; Euvrard, A.; Scahill, T. A. Heteronuclear Three-Dimensional NMR Spectroscopy of a Partially Denatured Protein: the A-state of Human Ubiquitin. *J. Biomol. NMR* **1993**, *3*, 285−296.
(52) Cox, J. P. L.; Evans, P. A.; Packman, L. C.; Williams, D. H.; Woolfson, D. N. Dissecting the Structure of a Partially Folded Protein Circular Dichroism and Nuclear Magnetic Resonance Studies of Peptides from Ubiquitin. *J. Mol. Biol.* **1993**, *234*, 483−492.
(53) Brutscher, B.; Brüschweiler, R.; Ernst, R. R. Backbone Dynamics and Structural Characterization of the Partially Folded A State of Ubiquitin by 1H, 13C, and 15N Nuclear Magnetic Resonance Spectroscopy. *Biochemistry* **1997**, *36*, 13043−13053.
(54) Cordier, F.; Grzesiek, S. Quantitative Comparison of the Hydrogen Bond Network of A-State and Native Ubiquitin by Hydrogen Bond Scalar Couplings. *Biochemistry* **2004**, *43*, 11295−11301.
(55) Kony, D. B.; Hünenberger, P. H.; van Gunsteren, W. F. Molecular Dynamics Simulations of the Native and Partially Folded States of Ubiquitin: Influence of Methanol Cosolvent, pH and Temperature on the protein Structure and Dynamics. *Protein Sci.* **2007**, *16*, 1101−1118.
(56) Pierson, N. A.; Chen, L.; Valentine, S. J.; Russell, D. H.; Clemmer, D. E. Number of Solution States of Bradykinin from Ion Mobility and Mass Spectrometry Measurements. *J. Am. Chem. Soc.* **2011**, *133*, 13810−13813.
(57) Silveira, J. A.; Fort, K. L; Kim, D. Y.; Servage, K. A.; Pierson, N. A.; Clemmer, D. E.; Russell, D. H. From Solution to the Gas Phase: Stepwise Dehydration and Kinetic Trapping of Substance P Reveals the Origin of Peptide Conformations. *J. Am. Chem. Soc.* **2013**, *135*, 19147−19153.
(58) Shi, H.; Pierson, N. A.; Valentine, S. J.; Clemmer, D. E. Conformation Types of Ubiquitin $[M + 8H]^{8+}$ Ions from Water:-Methanol Solutions: Evidence for the N and A States in Aqueous Solution. *J. Phys. Chem. B* **2012**, *116*, 3344−3352.
(59) Shi, H.; Gu, L.; Clemmer, D. E.; Robinson, R. A. S. Effects of Fe(II)/H2O2 Oxidation on Ubiquitin Conformers Measured by Ion Mobility-Mass Spectrometry. *J. Phys. Chem. B* **2013**, *117*, 164−173.
(60) Revercomb, H. E.; Mason, E. A. Theory of Plasma Chromatography/Gaseous Electrophoresis − A Review. *Anal. Chem.* **1975**, *47*, 970−983.
(61) Shvartsburg, A. A.; Jarrold, M. F. An Exact Hard-Spheres Scattering Model for the Mobilities of Polyatomic Ions. *Chem. Phys. Lett.* **1996**, *261*, 86−91.
(62) Dugourd, Ph.; Hudgins, R. R.; Clemmer, D. E.; Jarrold, M. F. High-Resolution Ion Mobility Measurements. *Rev. Sci. Instrum.* **1997**, *68*, 1122−1129.
(63) Hoaglund-Hyzer, C. S.; Clemmer, D. E. Ion Trap/Ion Mobility/Quadrupole/Time-of-Flight Mass Spectrometry for Peptide Mixture Analysis. *Anal. Chem.* **2001**, *73*, 177−184.
(64) Tang, K.; Shvartsburg, A. A.; Lee, H.-N..; Prior, D. C.; Buschbach, M. A.; Li, F.; Tolmachev, A. V.; Anderson, G. A.; Smith, R. D. High-Sensitivity Ion Mobility Spectrometry/Mass Spectrometry Using Electrodynamic Ion Funnel Interfaces. *Anal. Chem.* **2005**, *77*, 3330−3339.
(65) Koeniger, S. L.; Merenbloom, S. I.; Valentine, S. J.; Jarrold, M. F.; Udseth, H. R.; Smith, R. D.; Clemmer, D. E. An IMS-IMS Analogue of MS-MS. *Anal. Chem.* **2006**, *78*, 4161−4174.
(66) Katta, V.; Chait, B. T. Hydrogen/Deuterium Exchange Electrospray Ionization Mass Spectrometry: a Method for Probing Protein Conformational Changes in Solution. *J. Am. Chem. Soc.* **1993**, *115*, 6317−6321.
(67) Koeniger, S. L.; Clemmer, D. E. Resolution and Structural Transitions of Elongated States of Ubiquitin. *J. Am. Soc. Mass Spectrom.* **2007**, *18*, 322−331.